ISSN: 1355-0284 print / 1538-2443 online
DOI: 10.1080/13550280802008297

informa
healthcare

Up-regulation of chemokine gene transcripts and T-cell infiltration into the central nervous system and dorsal root ganglia are characteristics of experimental European bat lyssavirus type 2 infection of mice

KL Mansfield,[1] N Johnson,[1] A Nuñez,[1] D Hicks,[1] AC Jackson,[2] and AR Fooks[1]

[1]Rabies and Wildlife Zoonoses Group, Veterinary Laboratories Agency (VLA Weybridge), WHO Collaborating Centre for the Characterisation of Rabies and Rabies-Related Viruses, Addlestone, Surrey, United Kingdom; and [2]Departments of Internal Medicine (Neurology) and of Medical Microbiology, University of Manitoba, Winnipeg, Manitoba, Canada

European bat lyssaviruses (EBLV) types 1 and 2 are closely related to classical rabies virus (RABV), and are capable of causing rabies in terrestrial mammals, including humans. The authors have investigated the murine host innate immune response in the brain, salivary gland, spinal cord, and blood, following peripheral inoculation with EBLV-2. In the brain, increases in Toll-like receptor-3 (TLR-3) transcript preceded overt disease, with a range of inflammatory gene transcripts increasing during the clinical stage of infection. This included transcripts for interleukin-6 (IL-6), interferon-γ (IFN-γ), and CXC chemokine ligand 10 (CXCL10). In the salivary gland, there was a small but significant increase of CXCL10 gene transcript and a limited increase in 2′-5′ oligoadenylate synthetase (2′-5′ OAS1) transcript. In the blood, there was an increase in levels of IFN-γ and virus-neutralizing antibodies (VNAs) were detected prior to the appearance of clinical signs. These changes were associated with severe lymphocyte infiltration observed within the spinal cord and dorsal root ganglia (DRG), which was dominated by T lymphocytes and associated with widespread inflammatory changes. The authors speculate that the increase of inflammatory cytokines and chemokines in response to EBLV-2 infection leads to a dramatic increase in T-cell infiltration and provides evidence for a robust immune response to lyssavirus infection that may not commonly occur in RABV infection. *Journal of NeuroVirology* (2008) **14,** 218–228.

Keywords: bat; European; immune; lyssavirus; T cell

Introduction

The geographically restricted European bat lyssaviruses (EBLV) types 1 and 2 are closely related to classical rabies virus (RABV) and are classified within the genus *Lyssavirus*, family *Rhabdoviridae* (Nadin-Davis *et al*, 2007). Although they are detected in only a small number of bat species, they have been reported to cause rabies in terrestrial mammals, including humans (Fooks *et al*, 2003a). The Serotine bat (*Eptesicus serotinus*) is the reservoir host for EBLV type 1 (EBLV-1), and the Daubenton's bat (*Myotis daubentonii*) is the likely reservoir for EBLV type 2 (EBLV-2) (Fooks *et al*, 2004). In Great Britain, it has been reported that EBLV-2 is present at low levels within the native Daubenton's bat population (Brookes *et al*, 2005a). The presence of EBLV-2 in British bats poses a potential threat to both animal and human health, and has been diagnosed in one case of rabies in a

Address correspondence to A. R. Fooks, Rabies and Wildlife Zoonoses Group, Veterinary Laboratories Agency (VLA Weybridge), WHO Collaborating Centre for the Characterisation of Rabies and Rabies-Related Viruses, Woodham Lane, New Haw, Addlestone, Surrey, KT15 3NB, United Kingdom. E-mail: t.fooks@vla.defra.gsi.gov.uk

This study was funded by the Department for Environment, Food and Rural Affairs (DEFRA), UK (project SE0524).

Received 13 November 2007; revised 4 February 2008; accepted 18 February 2008.

bat rehabilitator in Scotland in 2002 (Fooks *et al*, 2003b).

Preliminary studies on EBLV-2 infection indicate that there is evidence for interferon (types 1 and 2) induction in response to neuroinvasion, but that this fails to control disease (Johnson *et al*, 2006). However, we have also observed that neuroinvasion with EBLV-2 is associated with the widespread development of inflammatory pathological changes within the brain, particularly the formation of perivascular cuffing, that may be more intense than with RABV infection. Furthermore, different studies have suggested that EBLV-2 shows diminished neurovirulence when directly compared to other lyssvirus genotypes (Vos *et al*, 2004; Brookes *et al*, 2007).

Previous work by our group has investigated the innate immune response in the murine model following peripheral infection with a 'street' strain of RABV, designated strain RV61, isolated from a human who contracted rabies from a dog bite in India (Johnson *et al*, 2008). This study demonstrated the up-regulation of a number of host mRNA transcripts in the brain and salivary gland, coincident with an increase in virus-specific neutralizing antibodies (VNAs), but with minimal lymphocytic infiltration into the central nervous system (CNS). These findings contrast with an earlier study where another street strain of RABV (fox isolate) infection induced an acute inflammatory response in the CNS (Jackson *et al*, 1989). Therefore, there appears to be variation in the host response elicited by different RABV strains, although various factors may contribute to these differences, including passage history of the viruses, dosage of inocula, inoculation route, or mouse strain used.

In this study, we have investigated the host inflammatory response to peripheral inoculation in the mouse model following challenge with EBLV-2. In particular, we have focused on Toll-like receptor 3 (TLR-3). This receptor is up-regulated during lyssavirus infection in an *in vitro* model (Préhaud *et al*, 2005) and is triggered in response to double-stranded RNA (dsRNA), an intermediary of viral replication that is specifically recognised by TLR-3, leading to the activation of nuclear factor (NF)-κB and production of type I interferons (IFNs) (Alexopoulou *et al*, 2001). Recently, it has been demonstrated that the RNA helicase retinoic acid–inducible protein I (RIG-I) is also involved in dsRNA-induced innate antiviral responses (Yoneyama *et al*, 2004). We have also focused on a number of other host transcripts, including interleukin (IL)-6, 2′-5′ oligoadenylate synthetase (2′-5′ OAS1, and IFN-γ, and in particular, two chemokines known to have chemotactic properties for T cells, CXCL10 (formerly IP-10) and CCL5 (RANTES), which have previously been shown to be expressed by microglia following infection with RABV (Nakamichi *et al*, 2005). The mouse model was deemed the most appropriate alternative to bats, as it provides a reliable and reproducible model of rabies virus–induced encephalitis, and enables us to study the immune response to infection. Peripheral challenge is the route of infection that most closely mimics the natural route of bite transmission. In addition, we have investigated the expression of a number of cytokine and chemokine gene transcripts in the brain and salivary gland that act to stimulate and coordinate the inflammatory response. This was compared to cytokine levels in the peripheral circulation to compare events both within and external to the CNS.

Results

Following peripheral inoculation with EBLV-2, the course of infection was variable and did not always result in the development of disease or demonstration of CNS invasion, as judged by the detection of viral RNA in the brain (Table 1). Clinical signs of infection, such as ruffled coat, reduced activity, and/or hind limb paralysis appeared between days 12 to 20 post inoculation (p.i.) (Table 1). For the purposes of data representation, mice were grouped according to the stage of infection: early ($n = 5$), preclinical ($n = 8$), and clinical ($n = 5$). The early time point was taken at the point of inoculation, whereas the preclinical and clinical time points were dictated by the appearance of clinical signs. Analysis by heminested reverse transcriptase–polymerase chain reaction (RT-PCR) demonstrated the presence of viral RNA in the brain by day 11 p.i., prior to the appearance of disease, during the preclinical stage of infection

Table 1 Time course of the murine EBLV-2 infection model

Stage of infection	Day post inoculation	Mouse ID	Clinical signs	Viral RNA (brain)	Viral RNA (salivary gland)
Early	0	0 + 1	−	−	−
	0	0 + 2	−	−	−
	0	0 + 3	−	−	−
	0	0 + 4	−	−	−
	0	0 + 5	−	−	−
Preclinical	11	11 + 1	−	+	−
	11	11 + 2	−	+	−
	11	11 + 3	−	+	−
	11	11 + 4	−	+	−
	11	11 + 5	−	−	−
	15	15 + 2	−	+	−
	15	15 + 3	−	+	−
	15	15 + 4	−	−	−
Clinical	12	12 + 1	+	+	+
	15	15 + 1	+	+	+
	17	17 + 1	+	+	+
	17	17 + 2	+	+	−
	20	20 + 1	+	+	−

Note. Parameters including the development of clinical disease and the presence of viral RNA in the brain and salivary gland are shown.

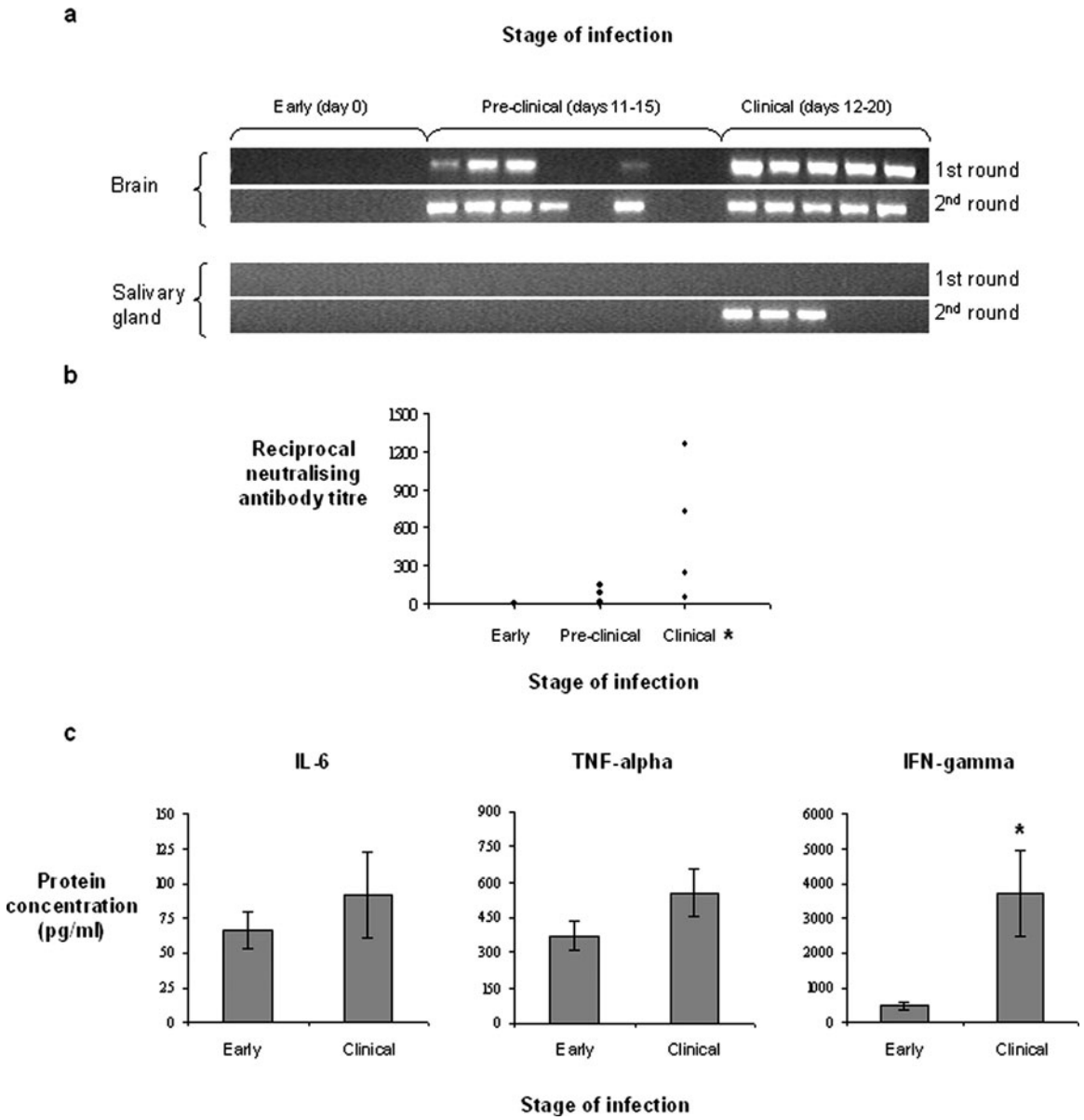

Figure 1 Time course of infection in a murine model of EBLV-2 disease. Numbers of mice used are as follows: early infection ($n = 5$), preclinical infection ($n = 8$), and clinical infection ($n = 5$). (**a**) Agarose gel demonstrating the detection of viral RNA by heminested RT-PCR in brain (*upper panels*) and salivary gland (*lower panels*) samples at defined points during the development of disease. Each lane represents a sample from an individual mouse. (**b**) Detection of neutralizing antibody in sera of mice inoculated with EBLV-2, immediately following inoculation (early), 11 to 15 days following inoculation (preclinical), and on the development of disease (clinical; between days 12 and 20 p.i.). Antibody was detected by the fluorescent antibody virus neutralisation test using homologous virus, and data is expressed as reciprocal neutralizing antibody titer. Values significantly different (unpaired *t* test, $p < .05$) from the day 0 value are marked (*). (**c**) Serology: transcriptional response to infection with EBLV-2 within the murine host-inflammatory cytokines IL-6, TNF-α, and IFN-γ. Host transcript analysis in the periphery was measured immediately (early; day 0 p.i.) and during development of disease (clinical; between days 12 and 20 p.i.) following infection with EBLV-2. Groups of mice were anesthetized and blood samples taken prior to being humanely killed. Serum samples were analyzed using a commercial microarray kit as described in Materials and Methods. Results are expressed as the mean protein concentration (pg/ml). Each bar shows the mean SEM of the group. Values significantly different (unpaired *t* test, $p <$ .05) from the day 0 value are marked (*).

(Figure 1a, Table 1). However, viral RNA was not detected in the salivary gland until clinical signs had developed, and even then only by nested PCR in three of five infected mice.

A reciprocal neutralizing antibody titer of >9 (as determined by virus neutralization) was considered to be evidence for seroconversion. This cut-off value of 9 was determined as a result of extensive work using a range of viruses in the mFAVN. Following infection with EBLV-2, circulating VNA were detected in the blood during the preclinical phase (days 5 to 11), coincident with the detection of viral RNA in the

brain, and prior to the appearance of clinical signs (Figure 1b). The mean reciprocal VNA titer increased from a baseline level of 0.58 to 34.78 at the intermediate time point, although this was not statistically significant ($p = .08$). However, by the clinical stage of infection, there was a significant increase ($p = .02$) in the reciprocal VNA titer to 570.36.

Cytokine protein microarray analysis of serum samples was used to demonstrate the acute phase response in the periphery. Key inflammatory cytokines IL-6, tumor necrosis factor (TNF)-α, and IFN-γ were all up-regulated by the clinical stage of EBLV-2 infection (Figure 1c). However, IFN-γ increased significantly ($p = .011$) between early and clinical infection. The observation of both VNA and increased serum IFN-γ suggest that peripheral immune activation had been stimulated in response to infection.

Following peripheral infection with EBLV-2, a number of transcriptional changes were observed within the brain (Figure 2a) and salivary gland (Figure 2b). Expression of TLR-3 mRNA transcript increased significantly over basal levels in the brain by preclinical infection ($p = .0012$) and prior to the appearance of clinical signs. Once clinical signs had appeared, this transcript increased 43-fold in the brain ($p = .027$). IL-6, an inflammatory cytokine, demonstrated a 74-fold increase in the brain during the clinical stage of infection, although this was not a statistically significant increase ($p = .057$). However, the apparent fall in IL-6 transcript in the salivary gland by clinical infection was significant ($p = .019$). Expression of mRNA transcript of the anti-viral protein 2′-5′ OAS1 was increased 12-fold in the brain by the preclinical stage of infection, and increased substantially by approximately 1800-fold in the brain by late-stage infection ($p = .0006$). Expression of this transcript increased transiently over basal levels in the salivary gland during preclinical infection, before decreasing by clinical infection. Transcripts for the chemokines CCL5 and CXCL10 both increased significantly in the brain by the clinical stage of infection; reaching 2100-fold for CCL5 and 2500-fold for CXCL10 ($p = .013$ and $p = .0001$, respectively). There was also a 6-fold increase in CCL5 mRNA transcript in the brain by preclinical infection ($p = .044$), although the 20-fold increase in CXCL10 transcript at the preclinical stage of infection was not significant. In the salivary gland, expression of CXCL10 transcript demonstrated a small continuous increase throughout the infection, with a 2.5-fold increase by preclinical infection and reaching a 5-fold increase by the clinical stage of infection over basal levels ($p = .023$). Expression of IFN-γ transcript was increased approximately 108-fold in the brain by clinical infection ($p = .0016$).

Mock-inoculation with tissue culture medium did not induce pathological changes within the spinal cord segments and dorsal root ganglia (DRG) (Figures 3a and 4a). Similarly, mice infected with EBLV-2 and killed immediately following inoculation did not demonstrate any inflammatory changes. EBLV-2–inoculated animals developed a moderate myelitis and a moderate to severe leptomeningitis from day 11 p.i. (Figure 3b, *arrows*), with marked diffuse and focal microgliosis with glial nodule formation and multiple perivascular cuffing observed in grey and white matter. These changes were more prominent in the thoracic segments of the spinal cord, and were accentuated by day 20 p.i. (Figure 3c, *arrows*). Perivascular cuffs were mainly lymphocytic and composed of only a few cells at day 11 p.i., whereas by day 20 p.i. they had become more prominent and cellular. The meningeal membranes also showed lymphocytic infiltration, especially in perivascular locations (Figure 3d).

In the DRG, mild to severe mononuclear ganglionitis, predominantly lymphocytic, was observed by day 11 p.i., along with degenerative changes in neurons, including central chromatolysis, nuclear margination, necrosis, and neuronophagia (Figure 4b to d). The lymphocytic infiltration was mainly located in the periphery of the ganglia and pachymeninges, and was observed to be more extensive in the lumbar ganglia than thoracic ganglia.

Immunolabeling of T and B cells using anti-CD3 and anti-CD45/B220 demonstrated that the composition of the lymphocytic infiltrates was a mixture of T and B cells in both the DRG and spinal cord sections, with T cells (Figure 5a and b) being more numerous than B cells in both compartments (Figure 5c and d). However, although the perivascular cuffs appear to be predominantly lymphocytic, it is possible that other mononuclear cell types including macrophages were present, particularly by day 20 p.i.

Discussion

Peripheral infection with EBLV-2 initiated a strong innate immune response, as evidenced by the increase in a range of inflammatory gene transcripts and coincident with a rapid humoral response in the form of the production of VNAs. The increase in cytokine and chemokine gene transcripts has also been observed following infection with RABV (Wang *et al*, 2005; Roy *et al*, 2007; Johnson *et al*, 2008). This contrasts with a previous report, which suggested that the predominant effect of RABV infection on host cells was gene down-regulation (Prosniak *et al*, 2001). It was also evident that following peripheral infection, viral RNA was detectable in the brain prior to the appearance of clinical signs in mice. Furthermore, CXCL10 transcripts increased in salivary gland tissue prior to the detection of virus in this organ. One possible stimulus for this response could be interferons generated by infected cells at the site of inoculation or the spinal cord for the purpose of limiting virus replication (Haller *et al*, 2006) and, indeed, INF-γ was observed in the serum of infected mice (Figure 1c). VNAs were also detected early in the course of infection suggesting

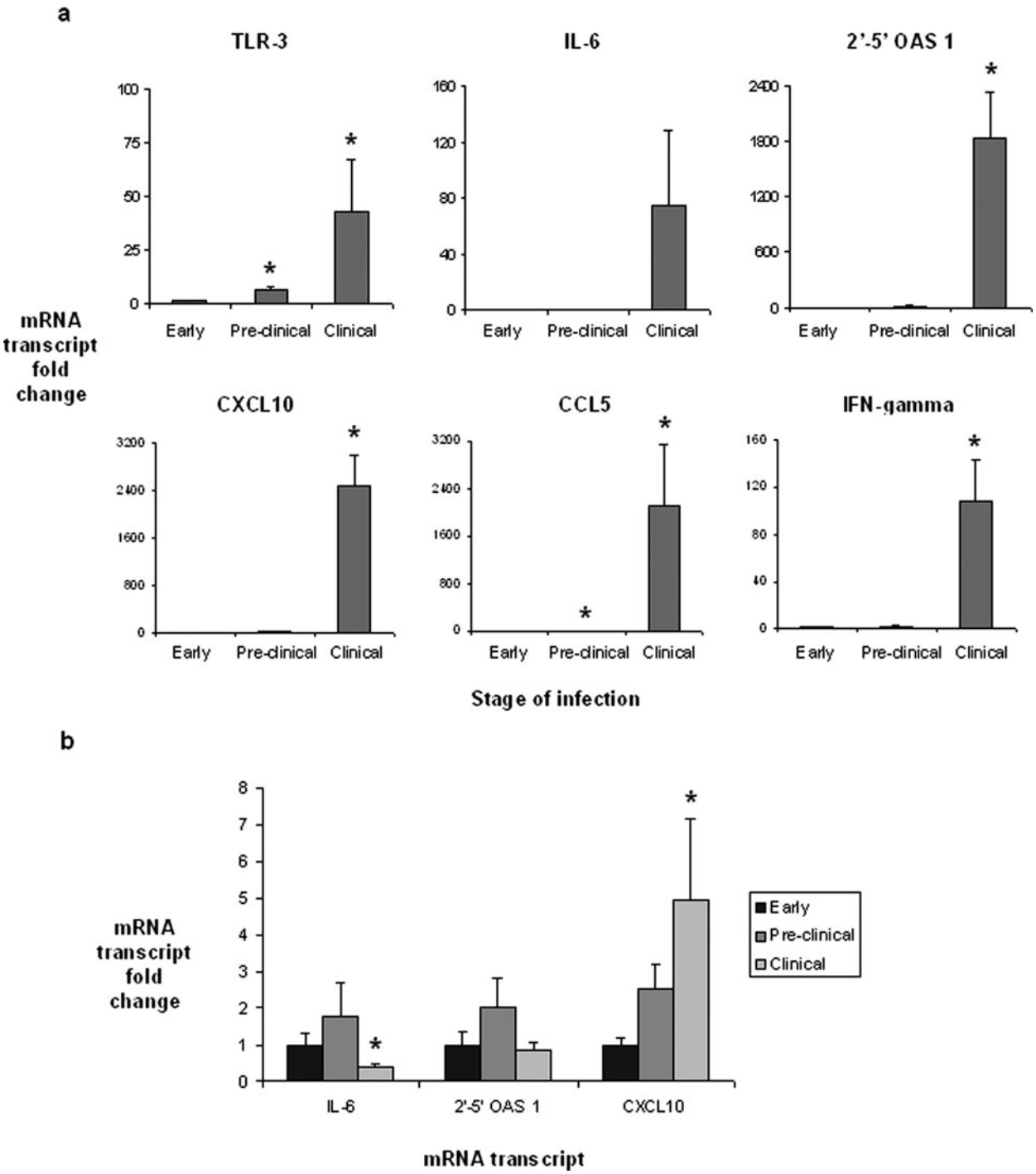

Figure 2 Host transcriptional response to infection with EBLV-2 within the murine host, in the brain (**a**) and salivary gland (**b**). Fold change of mRNA transcripts TLR-3, IL-6, 2′-5′OAS1, CXCL10, CCL5, and IFN-γ were measured immediately (early), prior to disease (preclinical) and during the development of disease (clinical), following infection with EBLV-2. Numbers of mice used are as follows: early infection ($n = 5$), preclinical infection ($n = 8$), and clinical infection ($n = 5$). Groups of mice were humanely killed and organ samples removed immediately. Total RNA was extracted and treated as described in Materials and Methods. Results are expressed as fold change over the early (baseline) sample. Each bar shows the mean SEM of the group, and values significantly different (unpaired t test, $p < .05$) from the day 0 value are marked (*).

early initiation of the humoral response. However, neither the early innate response nor the VNAs appear to have limited the spread of virus within the CNS.

We have also demonstrated that infection with EBLV-2 induced an early increase in TLR-3 gene expression within the CNS, which correlated with the detection of viral RNA. This agrees with observations

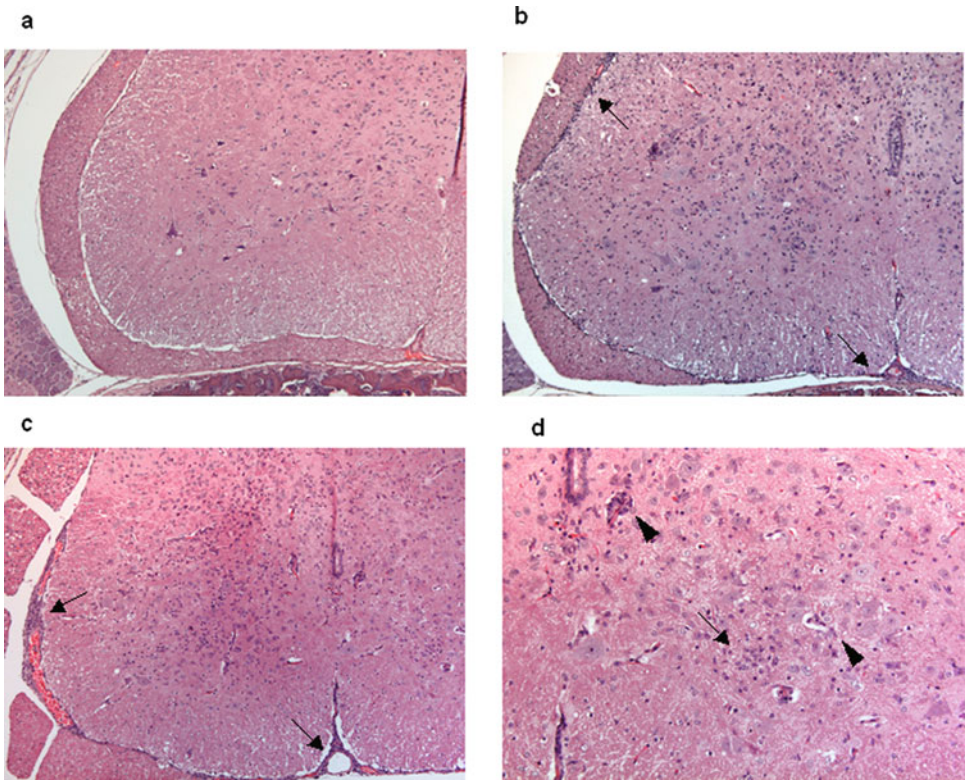

Figure 3 Hematoxylin and eosin–stained section: pathology of EBLV-2 infection within the spinal cord following hind limb footpad inoculation with virus. (**a**) A section of thoracic spinal cord, control (10×; medium inoculated) showing normal histology. (**b**) A section of thoracic spinal cord (10×; preclinical, day 11 p.i.) showing moderate diffuse and focal microgliosis and mononuclear infiltration in the leptomeninges (*arrows*). (**c**) A section of thoracic spinal cord (10×; clinical, day 20 p.i.) showing moderate diffuse and focal microgliosis and mononuclear infiltration in the leptomeninges (*arrows*). (**d**) Detail of **c** (20×), showing glial nodule formation (*arrow*) and perivascular cuffing (*arrowheads*).

by ourselves and others of TLR-3 activation within models of RABV infection (McKimmie *et al*, 2005; Préhaud *et al*, 2005) that activation of this receptor is an early marker of the innate immune response to lyssavirus infection, and also occurs in human rabies encephalitis (Jackson *et al*, 2006). However, an alternative receptor signaling system has been identified involving the retinoic acid–inducible protein I (RIG-I), which also induces interferon in response to RABV. This mechanism functions through direct recognition of genomic RNA rather than dsRNA derived from viral replication (Hornung *et al*, 2006). In addition to the induction of an antiviral immune response, there is evidence that suggests TLRs may participate in pathogenesis (Sen and Sarker, 2005). Our data show increases in IL-6 gene transcription in the brain, although this is not reflected in changes of serum IL-6, suggesting that any role this cytokine plays in the inflammatory response is limited to the CNS.

Previous studies have demonstrated that infection with RABV strongly induced microglial expression of the CXCL10 and CCL5 (Nakamichi *et al*, 2005). A receptor for CXCL10, CXCR3, has been shown to be expressed on T-helper cells type 1 (Th1) (Bonecchi *et al*, 1998), implicating CXCL10 in the T-cell response to infection. Thus, chemokines appear to have a proinflammatory role that is often associated with a Th1 cytokine expression profile (IFN- γ) and, therefore, with a Th1 cell infiltrate at the site of inflammation (Rossi and Zlotnik, 2000). Our data support this for lyssavirus infection, with the demonstration of increases in CCL5, CXCL10, and IFN- γ transcripts in the brain coinciding with the appearance of disease and recruitment of T cells into the CNS. In comparison, in previous studies we have shown that following similar inoculation experiments with street strain RABV, both CXCL10 and IFN-γ gene transcripts were elevated in the brain and some limited T-cell infiltration was observed (Johnson *et al*, 2008). However, the extent of lymphocytic infiltration in the spinal cord and DRG was reduced and there was no evidence of pathological changes within the brain that are a common feature of EBLV-2 infection (data not shown). Neuronophagia was observed in the DRG by the time clinical signs had appeared on day 11 p.i. This observation agrees with earlier studies with RABV that observed few histological changes in the brain, in comparison to attenuated RABV, which induced inflammation, perivascular cuffing, and infiltration of macrophages and lymphocytes (Wang *et al*, 2005). However, this is in direct contrast to earlier work,

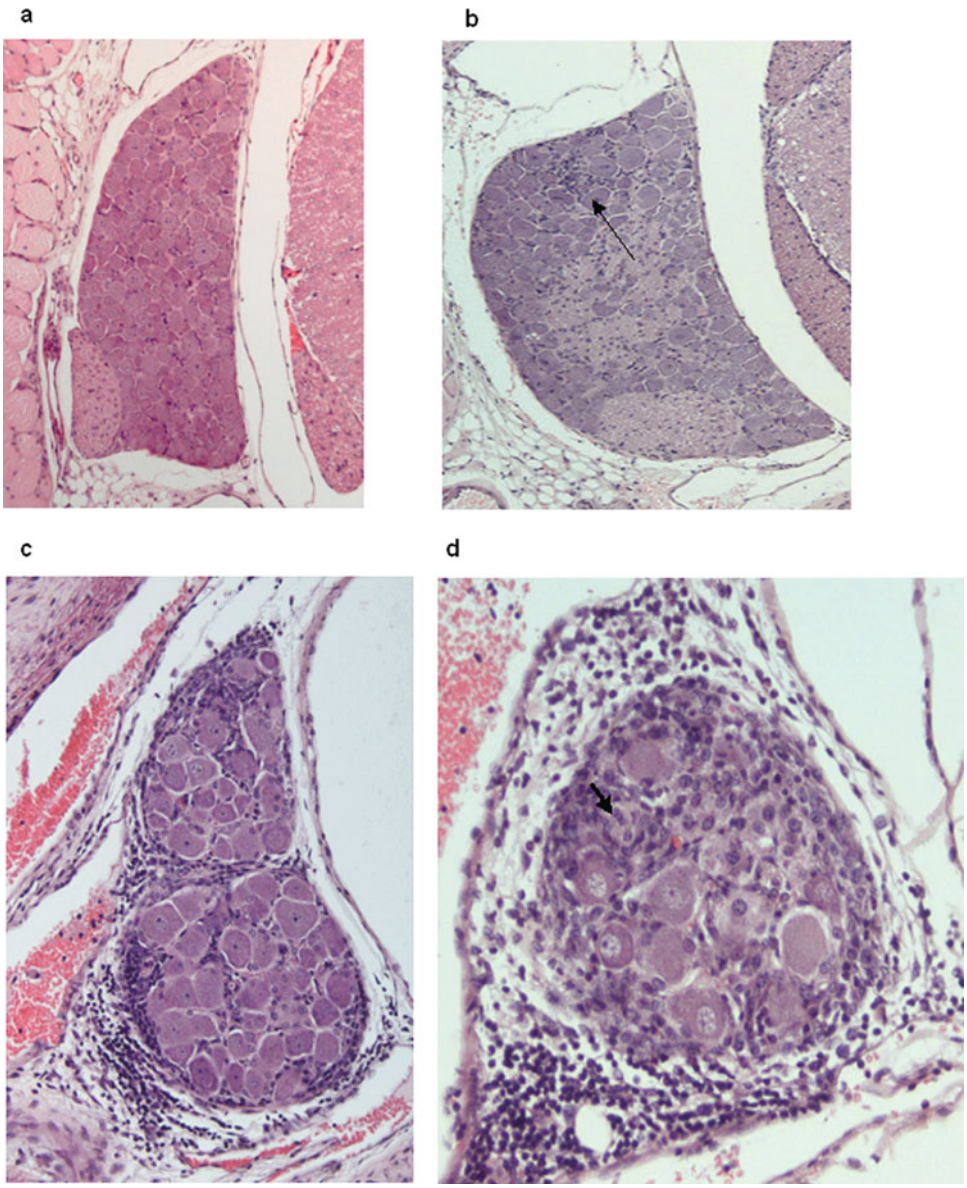

Figure 4 Hematoxylin and eosin–stained section: pathology of EBLV-2 infection within the dorsal root ganglia following footpad inoculation with virus. (**a**) A section of a dorsal root ganglion, thoracic, control (10×; medium inoculated) showing normal histology. (**b**) A section of a dorsal root ganglion, thoracic (10×; preclinical, day 11 p.i.) showing mild mononuclear ganglionitis and neuronophagia (*arrow*). (**c**) A section of a dorsal root ganglion, lumbar (20×; preclinical, day 11 p.i.) showing mononuclear ganglionitis and lymphocytic infiltration of the dorsal root ganglion and peripheral tissue. (**d**) A section of a dorsal root ganglion, lumbar (20×; preclinical, day 11 p.i.) showing mononuclear ganglionitis with central chromatolysis of neurons, nuclear margination, and neuronophagia of neurons with surrounding inflammatory cells. A neuronophagic nodule containing a group of concentric cells (nuclei), which have phagocytosed and replaced a neuron (*arrow*).

where peripheral inoculation of mice with a street strain RABV induced an acute inflammatory reaction in the CNS, which included perivascular cuffing within the spinal cord and DRG, but limited degeneration of neurons (Jackson *et al*, 1989). Therefore, it is clear that following infection with a rabies virus, the extent of the histopathological changes observed can vary considerably with the particular strain of rabies virus. However, as previously mentioned, possible factors that may contribute to these differences include the use of different strains of mouse, or differences in the passage history of the viruses used. Furthermore, future work should focus on the characterisation of infiltrating mononuclear cells to elucidate the likely impact on the CNS of each cell type.

In the murine model, the high magnitude transcriptional response does not occur until the clinical stage of infection, at a point where the immune response fails to control infection. Following EBLV-2 infection, the substantial host innate immune response was still insufficient to control infection and prevent a fatal outcome. Perivascular infiltration of T cells has

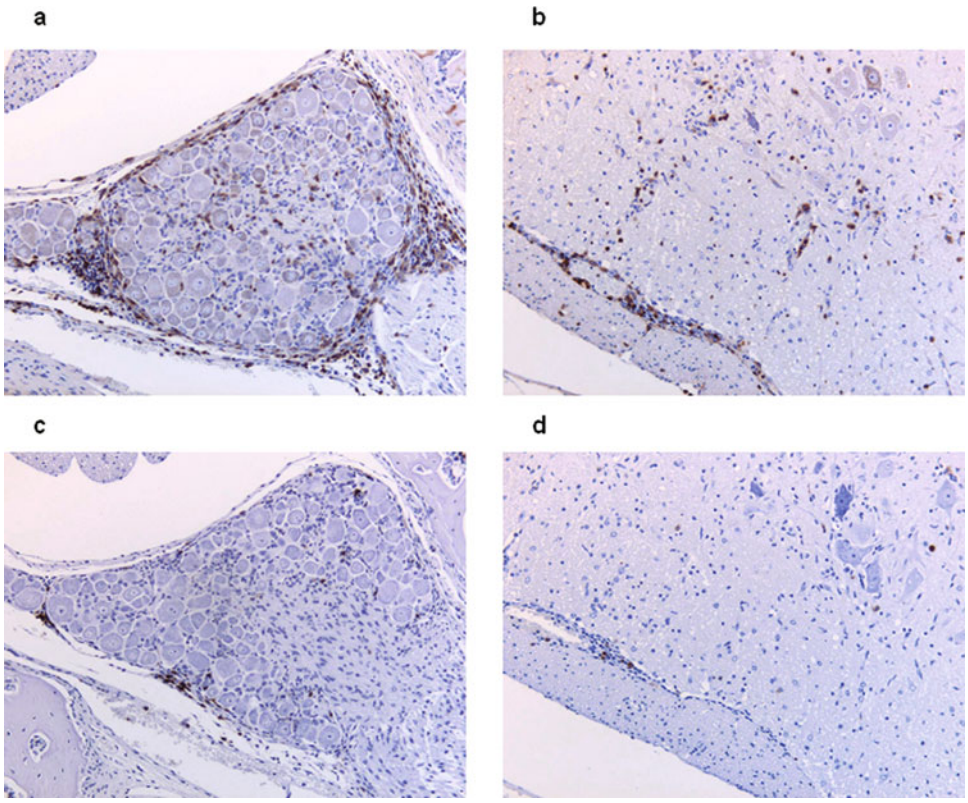

Figure 5 Immunohistochemical detection of CD3 T lymphocytes (**a** and **b**) and CD45R/B220 B-lymphocytes (**c** and **d**), in serial sections of dorsal root ganglia (20×; day 11 p.i.) and spinal cord (20×; day 20 p.i.). Lymphocytic infiltrates are predominantly composed of T cells.

also been associated directly with the development of paralysis in mice infected with RABV (Sugamata *et al*, 1992), suggesting a further negative outcome of T-cell infiltration of the spinal cord in response to EBLV-2 infection.

There is evidence that evasion of the immune response occurs via viral IFN antagonists, which interfere with the activation of type 1 interferons (Wang *et al*, 2005). Recently, *Lyssavirus* antagonists have been identified, that impair the IFN-α/β system by interfering with pathways that activate interferon regulatory factors (IRF) IRF-3 and IRF-7 (Conzelmann, 2005). It has been suggested that the rabies virus phosphoprotein interferes with the activation of IRF-3 (Brzózka *et al*, 2005), and the phosphoprotein of EBLV-2 may act in a similar manner. However, we and others have observed increases in a range of interferon-inducible genes during lyssavirus infection suggesting that inhibition does not limit transcription. Some of the induced transcripts, including CXCL10 and IFN-γ could enhance T-cell infiltration with both positive and negative consequences for the host.

Materials and methods

Challenge virus

EBLV-2 (strain RV1332) was isolated from the brain of a Daubenton's bat (*Myotis daubentonii*) in the United Kingdom (Johnson *et al*, 2003). Virus stocks were grown to a titer of 3×10^5 $TCID_{50}$/ml in N2a neuroblastoma cells following three passages in mice.

Mouse inoculations

Groups of five female outbred CD1 mice were inoculated with 30 μl of virus culture supernatant in the left hindlimb footpad under isoflurane anesthesia. Uninfected control mice were inoculated with medium only. At specific time points or on the development of disease, groups were euthanized. Mice were anesthetized, and subject to a terminal bleed by cardiac puncture. From every mouse, the brain and salivary glands (submaxillary and parotid) were removed. The vertebral column was removed from selected mice on days 0, 11, and 20 p.i. Control mice were sacrificed on day 0 post inoculation (p.i.) and day 25 p.i. Cardiac perfusion was not used during the extraction of organs from mice, and it is possible that small amounts of blood were unavoidably harvested at the same time as the brain and salivary gland. However, the contribution of RNA from this source compared to that derived from the whole organ (brain or salivary gland) would be insignificant.

Histopathology and immunohistochemistry

Vertebral columns were fixed in 10% neutral-buffered formalin for a minimum of 5 days. Formalin-fixed tissues were transferred to a 12.5% pH 7 EDTA

(disodium) solution (Sigma-Aldrich, USA) for decalcification during 2 weeks and were blocked and processed routinely to paraffin wax. Serial 4-μm wax sections were cut and stained with hematoxylin and eosin for histopathogical examination or used for immunohistochemistry.

Identification of T and B lymphocytes in tissue sections was performed by immunohistochemistry, using a CD3 pan T-cell marker or CD45R/B220 B-cell marker, respectively. Briefly, 4-μm sections were dewaxed in xylene, and passed through graded alcohols to Tris-buffered saline solution (TBS) (0.005 M Tris, pH 7.6, 0.85% NaCl). Endogenous peroxidase activity was quenched with a methanol/hydrogen peroxide block (BDH) for 15 min. Slides were assembled into Shandon coverplates to facilitate immunohistochemistry (IHC) using the Shandon Sequenza system (Shandon, USA) and primary antibody cross-reactivity with tissue constituents was blocked using normal serum. Samples were subsequently incubated with either rat anti-mouse CD45R/B220 (BD Pharmigen) (1:50) or rabbit anti-human CD3 (Dako) (1:500) primary antibodies, overnight at 4°C. Either biotinylated rabbit anti-rat immunoglobulin (Ig) or goat anti-rabbit secondary antibody, respectively, was incubated for 30 min at room temperature, followed by avidin-biotin-peroxidase conjugate (ABC^{elite} Vector Laboratories) for 30 min. Sections were washed three times with TBS between incubations. The immunohistochemical signal was visualised using 3,3'-diaminobenzidine (Sigma-Aldrich), and sections were counterstained in Mayer's hematoxylin (Surgipath, UK), dehydrated in absolute alcohol, cleared in xylene, and coverslipped.

Modified fluorescent antibody virus neutralization assay (mFAVN) and microarray

Blood samples were centrifuged and the serum removed, before being heat inactivated at 56°C for 30 min. Serum samples were then tested by mFAVN using homologous virus to that used to inoculate the mice. This followed the modifications of the existing FAVN technique (Brookes *et al*, 2005b). Protein microarray analysis of the serum samples was undertaken using the ProteoPlex 16-well murine cytokine array (Novagen), following the manufacturer's protocol. Scanning and analysis were performed by the manufacturer.

RNA extraction, reverse transcription, and PCR amplification

Total RNA was extracted from organ samples, using TRIzol (Invitrogen) following standard protocols. Extracted RNA was resuspended in high-performance liquid chromatography (HPLC)-purified water and treated with 0.3 units/μl DNase using the RNeasy Mini Kit (Qiagen) following the manufacturer's instructions. RNA quality and quantity was then assessed using a ND-1000 spectrophotometer (Nanodrop) and diluted to a final concentration 1 μg/μl in HPLC water.

To confirm the presence of virus in the brain and salivary glands, RNA samples were reverse transcribed with the primer JW12 (ATGTAACACCYCTACAATG), and then amplified using a previously published hemi-nested PCR (Heaton *et al*, 1997). Murine mRNA transcripts were detected by reverse transcription with Moloney murine leukemia virus reverse transcriptase (M-MLV RT) and the Oligo dT_{15} primer, in the presence of 14 units of RNAsin and 10 mM dithiothreitol, with incubation for 60 min at 42°C. Amplification using transcript-specific primer sets was performed using SYBR Green JumpStart Taq Readymix (Sigma Aldrich) and a Mx3000p (Stratagene). Amplification was achieved using specific primers for IL-6, TLR-3, 2′-5′ OAS1, IFN-γ, CCL5, CXCL10, and β-actin, and the sequence of each primer combination is detailed in Table 2. Each mRNA transcript was quantified by comparison with a standard curve, and β-actin transcript was used to normalize each transcript within the sample. Transcript fold changes were calculated relative to the zero time point (day 0 post infection) (McKimmie *et al*, 2005).

Table 2 Primers used in this study

Transcript	Primer	Sequence	Tm (°C)	Source
IL6	IL6 for	CTCTGGTCTTCTGGAGTWC	56.3	This study
	IL6 rev	CCACAGTGAGGAATGTCC	58.9	
2′-5′-OAS 1	OAS1 for	CTGASCTTCAAGCTGAGC	56	This study
	OAS1 rev	CAGCTTCTCCTTACACAGTTG	59.1	
TLR-3	TLR3 for 2	CCAGGAATGGAGAGGTC	57.9	This study
	TLR3 rev 2	GATGTGGAGGTGAGACAG	56.2	
CCL5	CCL5 for	TCTCTGCAGCTGCCCTCACC	70.4	Lacroix-Lamandé *et al*, 2002
	CCL5 rev	TGGGAGTAGGGGATTACTGAGT	62.5	
CXCL10	CXCL10 for	ATGAACCCAAGTGCTGCCGTC	70.5	Lacroix-Lamandé *et al*, 2002
	CXCL10 rev	TGGAGAGACAGGCTCTCTGCT	65.7	
INF-γ	INF-γ 1	AGCGGCTGACTGAACTCAGATTGTAG	69.4	This study
	INF-γ 2	GTCACAGTTTTCAGCTGTATAGGG	62.6	
β-Actin	β−Actin 1	TGGAATCCTGTGGCATCCATGAAAC	73.2	Murray *et al*, 1990
	β-Actin 2	TAAAACGCAGCTCAGTAACAGTCCG	68.8	

References

Alexopoulou L, Holt AC, Medzhitov R, Flavell R (2001). Recognition of double-stranded RNA and activation of NF-κB by Toll-like receptor 3. *Nature* **413:** 732–738.

Bonecchi R, Bianchi G, Bordignon PP, D'Ambrosio D, Lang R, Borsatti A, Sozzani S, Allavena P, Gray PA, Mantovani A, Sinigaglia F (1998). Differential expression of chemokine receptors and chemotactic responsiveness of Type 1 T helper cells (Th1s) and Th2s. *J Exp Med* **187:** 129–134.

Brookes SM, Aegerter JN, Smith GC, Healy D., Joliffe TA, Swift SM, Mackie IJ, Pritchand JS, Pacey PA, Moore NP, Focks AK (2005a). European bat lyssaviruses in Scottish bats. *Emerg Infect Dis* **11:** 572–578.

Brookes SM, Klopfleisch R, Muller T, Healy DM, Teifke J, Lange E, Kliemt J, Johnson N, Finnegan CJ, Johnson L, Kaden V, Vos A Fooks, AR (2007). Susceptibility of sheep to European bat lyssavirus types 1 and 2 infection: A clinical pathogenesis study. *Vet Microbiol* **125:** 210–223.

Brookes SM, Parsons G, Johnson N, McElhinney LM, Fooks AR (2005b). Rabies human diploid vaccine elicits cross-neutralizing and cross-protecting immune responses against European and Australian bat lyssaviruses. *Vaccine* **23:** 4101–4109.

Brzózka K, Finke S, Conzelmann K-K (2005). Identification of the rabies virus alpha/beta interferon antagonist: phosphoprotein P interferes with phosphorylation of interferon regulatory factor 3. *J Virol* **79:** 7673–7681.

Conzelmann K-K (2005). Transcriptional activation of alpha/beta interferon genes: interference by nonsegmented negative-strand RNA viruses. *J Virol* **79:** 5241–5248.

Fooks AR, Brookes SM, Johnson N, McElhinney LM, Hutson AM (2003a). Review article: European bat lyssaviruses: an emerging zoonoses. *Epidemiol Infect* **131:** 1029–1039.

Fooks AR, McElhinney LM, Marston DA, Selden D, Joliffe TA, Wakeley PR, Johnson N, Brookes SM (2004). Identification of a European bat lyssavirus type 2 in a Daubenton's bat found in Staines, Surrey, UK. *Vet Rec* **155:** 434–435.

Fooks AR, McElhinney LM, Pounder DJ, Finnegan CJ, Mansfield K, Johnson N, Brookes SM, Parsons G, White K, McIntyre PG, Nathwani D (2003b). Case report: Isolation of a European bat lyssavirus type 2a from a fatal human case of rabies encephalitis. *J Med Virol* **71:** 281–289.

Haller O, Kochs G, Weber F (2006). The interferon response circuit: Induction and suppression by pathogenic viruses. *Virology* **344:** 119–130.

Heaton PR, Johnstone P, McElhinney LM, Cowley R, O'Sullivan E, Whitby JE (1997). Heminested PCR assay for detection of six genotypes of rabies and rabies-related viruses. *J Clin Microbiol* **35:** 2762–2766.

Hornung V, Ellegast J, Kim S, Brzózka K, Jung A, Kato H, Poeck H, Akira S, Conzelmann K-K, Schlee M, Endres S, Hartmann G (2006). 5'-Triphosphate RNA is the ligand for RIG-I. *Science* **314:** 994–997.

Jackson AC, Reimer DL, Ludwin SK (1989). Spontaneous recovery from the encephalomyelitis in mice caused by street rabies virus. *Neuropathol Appl Neurobiol* **15:** 459–475.

Jackson AC, Rossiter JP, Lafon M (2006). Expression of Toll-like receptor 3 in in the human cerebellar cortex in rabies, herpes simplex encephalitis, and other neurological diseases in humans. *J NeuroVirol* **12:** 229–234.

Johnson N, Mansfield KL, Hicks D, Nunez A, Healy D, Brookes SM, McKimmie CS, Fazakerley J K, Fooks AR (2008). Inflammatory responses in the nervous system of mice infected with a street isolate of rabies virus. In Towards the Elimination of Rabies in Eurasia. Dev Biol 131. Doclet B, Fooks AR, Müller T, Torclo N, Scientific and Technical Department of the OIE (eds). Karger, Basel, pp. 65–72.

Johnson N, McKimmie CS, Mansfield KL, Wakeley PR, Brookes SM, Fazakerley JK, Fooks AR (2006). Lyssavirus infection activates interferon gene expression in the brain. *J Gen Virol* **87:** 2663–2667.

Johnson N, Selden D, Parsons G, Healy D, Brookes SM, McElhinney LM, Hutson AM, Fooks AR (2003). Isolation of a European bat lyssavirus type 2 from a Daubenton's bat in the United Kingdom. *Vet Rec* **152:** 383–387.

Lacroix-Lamandé S, Mancassola R, Naciri M, Laurent F (2002). Role of gamma interferon in chemokine expression in the ileum of mice and in a murine intestinal epithelial cell line after *Cryptosporidium parvum* infection. *Infect Immun* **70:** 2090–2099.

McKimmie CS, Johnson N, Fooks AR, Fazakerley JK (2005). Viruses selectively upregulate Toll-like receptors in the central nervous system. *Biochem Biophys Res Commun* **336:** 925–933.

Murray LJ, Lee R, Martens C (1990). *In vivo* cytokine gene expression in T cell subsets of the autoimmune MRL/Mp-*lpr/lpr* mouse. *Eur J Immunol* **20:** 163–170.

Nadin-Davis SA (2007). Molecular epidemiology. In: *Rabies,* 2 ed. Jackson AC, Wunner WH (eds). *London: Elsevier Academic Press* pp 69–122.

Nakamichi K, Saiki M, Sawada M, Takayama-Ito M, Yamamuro Y, Morimoto K, Kurane I (2005). Rabies virus-induced activation of mitogen-activated protein kinase and NF-κB signalling pathways regulates expression of CXC and CC chemokine ligands in microglia. *J Virol* **79:** 11801–11812.

Préhaud C, Mégret F, Lafage M, Lafon M (2005). Virus infection switches TLR-3-positive human neurons to become strong producers of beta interferon. *J Virol* **79:** 12893–12904.

Prosniak M, Hooper DC, Dietzschold B, Koprowski H (2001). Effect of rabies virus infection on gene expression in mouse brain. *Proc Natl Acad Sci U S A* **98:** 2758–2763.

Rossi D, Zlotnik A (2000). The biology of chemokines and their receptors. *Ann Rev Immunol* **18:** 217–242.

Roy A, Phares TW, Koprowski H, Hooper DG (2007). Failure to open the blood-brain barriers and deliver immune effectors to central nervous system tissues leads to the lethal outcome of silver-haired bat rabies virus infection. *J Virol* **81:** 1110–1118.

Sen GC, Sarker SN (2005). Transcriptional signalling by double-stranded RNA: role of TLR3. *Cytokine Growth Factor Rev* **16:** 1–14.

Sugamata M, Miyazawa M, Mori S, Spangrude GJ, Ewalt LC, Lodmell DL (1992). Paralysis of street rabies

virus-infected mice is dependent on T lymphocytes. *J Virol* **66:** 1252–1260.

Vos A, Muller T, Cox J, Neubert L, Fooks AR (2004). Susceptibility of ferrets (Mustela putorius furo) to experimentally induced rabies with European bat lyssaviruses (EBLV). *J Med Vet B Infect Dis Vet Pub Health* **51:** 55–60.

Wang ZW, Sarmento L, Wang Y, Li X-Q, Dhingra V, Tseggai T, Jiang B, Fu ZF (2005). Attenuated rabies virus activates, while pathogenic rabies virus evades, the host innate immune responses in the central nervous system. *J Virol* **79:** 12554–12565.

Yoneyama M, Kikuchi M, Natsukawa T, Shinobu N, Imaizumi T, Miyagishi M, Taira K, Akira S, Fujita T (2004). The RNA helicase RIG-I has an essential function in double-stranded RNA-induced innate antiviral responses. *Nature Immunol* **5:** 730–737.